Scientia Iranica B (2017) 24(1), 164–182

Sharif University of Technology
Scientia Iranica
Transactions B: Mechanical Engineering
www.scientiairanica.com

Ground motion prediction equation for inelastic spectral displacement in Iran

N. Hassani[a,*], G. Ghodrati Amiri[b], M. Bararnia[a] and F. Sinaeian[c]

a. *Abbaspour College of Engineering, Shahid Beheshti University, Tehran, Iran.*
b. *School of Civil Engineering, Iran University of Science & Technology, Tehran, Iran.*
c. *Building and Housing Research Center, Tehran, Iran.*

Received 14 October 2014; received in revised form 15 November 2015; accepted 16 April 2016

KEYWORDS
Ground-motion prediction equation;
Inelastic spectrum;
Inelastic displacement;
Iran.

Abstract. This paper is devoted to investigating the inelastic displacement spectra compatible with Iran. Owing to inadequacy of code-compliant elastic design spectra to predict structural damage during sever earthquakes, different approaches are proposed to overcome this problem. Inelastic design spectrum is one of the most well-known methods introduced by researchers. In practice, attenuation relationships can be used in probabilistic seismic hazard analysis to obtain the inelastic design spectrum. In this paper, a new Ground Motion Prediction Equation (GMPE) has been proposed for inelastic spectral displacement. In this regard, 806 horizontal ground motions are utilized with magnitudes ranging from 4 to 7 and epicentral distances less than 200 Km, which are obtained from 330 earthquakes in Iran. According to the tectonic condition, Iran zone can be divided into two parts: Zagros and Alborz-central Iran. However, three equations have been presented for the whole country zone, Zagros and Alborz-central Iran zones, separately. The main parameters such as earthquake magnitude, site-source distance, and site conditions have been related to the inelastic spectral displacement. Based on average shear wave velocity to a depth of 30 m, sites have been categorized into three classes. For the purpose of practicality, simplified equations have been proposed to predict inelastic spectral displacements in Iran.

1. Introduction

Currently, elastic design spectra, considered as an important part of earthquake engineering, are widely used in design process of structures. However, during severe earthquakes, structures do not remain elastic and behave inelastically. It is obvious that, generally, designing structures to remain elastic at moderated and high risk levels is not economically reasonable.

Most seismic design provisions allow structures to behave inelastically and dissipate earthquake input energy through hysteretic behavior of their structural elements during moderate and sever earthquakes.

Elastic design spectrum has many limitations such as predicting structural damage during severe earthquakes and considering the effects of inelastic behavior on seismic demand of structures. Inelastic spectrum compared to the elastic spectrum has two main advantages: (a) energy absorption due to hysteretic behavior and (b) increase of structural period due to decrease of lateral stiffness [1], as shown in Figure 1. Tothong and Cornell [2] proposed an empirical ground motion attenuation relation to estimate the inelastic displacement ratio. Unlike the previous studies, such as those were conducted by Ruiz-García and Miranda [3,4] and Miranda [5], Tothong and Cornell [2] proposed a new equation for inelastic displacement ratio as a function of earthquake magnitude. They used 291 strong ground motions from

*. *Corresponding author. Tel.: +98 21 77006661*
E-mail address: n_hassani@sbu.ac.ir (N. Hassani)

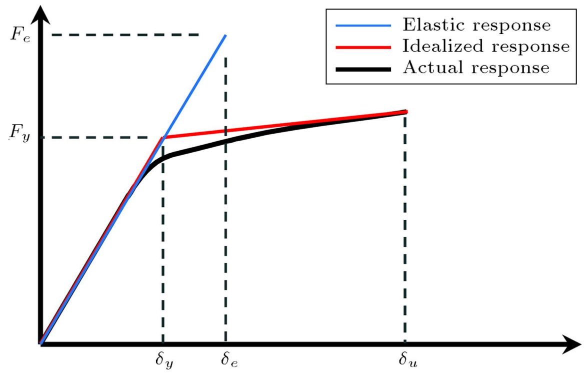

Figure 1. Force-deformation characteristics of linear and simplified nonlinear single-degree-of-freedom systems.

28 historical earthquakes with moment magnitudes of 5.65–7.9.

Tothong and Cornell [2] proposed a model that included these steps: At first, elastic displacement could be estimated by use of elastic Ground Motion Perediction Equation (GMPE). At the second step, inelastic displacement ratio would be obtained by the proposed equation. Finally, inelastic displacement could be estimated by multiplying the values of the first and second steps. Their equation can be used to estimate inelastic displacement of structures with known yield displacement (d_y).

Bozorgnia et al. [1] proposed a GMPE for inelastic response spectra. They used 3100 horizontal ground motions recorded in 64 earthquakes with moment magnitudes ranging in 4.3-7.9. Their results are based on constant ductility inelastic spectrum. The main advantage of the proposed equation is that the elastic response spectrum does not need to be computed.

This paper introduces the steps to determine an attenuation relation for inelastic spectral displacement that could be used in both deterministic and probabilistic seismic hazard analyses [6]. To this end, a GMPE is developed for estimation of inelastic spectral displacement, in which computing the corresponding elastic response spectrum will not be mandatory. Furthermore, for the structures in which $p - \Delta$ effects are negligible, the proposed relation could be used for calculating target displacement in pushover analysis. In this paper, the attenuation relations have been proposed different from those presented in previous models.

The main difference is that most of the old models have been designed for oscillators with constant ductility [1;5], while here we do not need to obtain a prespecified level of ductility in the design step [2]. However, the main objective is to evaluate the behavior of an oscillator with specific structural characteristics such as F_y. This new GMPE will be particularly useful in evaluating the performance of existing structures. Also, Ruiz-García and Miranda [3] note that if the inelastic displacement ratio, which is obtained from a constant ductility spectrum, is used for evaluating inelastic displacement of systems with known lateral strength, the resulting values for the maximum response would be underestimated. This new investigation is in continuation of the previous research conducted by the second author on the subject of attenuation relationships in Iran [7,8].

2. Earthquake data and modifications

The process of data selection depends on several parameters such as quality of records, magnitude, distance, site type, causative fault, etc. Based on device type, registered data in Iran are classified into two categories, analogue (SMA1) and digital classes (SSA2). Some of the registered data, which were recorded by analogue devices before 1994, have low quality and are disregarded in order to avoid any probable errors.

Nowadays, moment magnitude scale is used in ground motion prediction equations. One of the main reasons is the fact that it is not saturate in intense events. The moment magnitude scale of the most recent events has been reported in Iran's earthquakes catalogues, but it has not been reported for most events that occurred before 1994. Hence, in the proposed relation, the moment magnitude scale has been used and empirical relations are used in order to convert other magnitudes to the moment magnitude [9-11]. The magnitudes of the selected earthquakes range from 4 to 7.3.

Depending on whether the type of seismic source is point or finite, there are several criteria to measure source-to-site distance. Unfortunately, due to the lack of information about causative faults, only epicenter distance and focal depth parameters have been reported in Iran's earthquakes catalogues [12]. In order to obtain Hypocentral distance, researchers can use focal depth and epicenter values. Hypocentral distance is assumed to be the hypotenuse of a right triangle in which focal depth and epicenter distances are the other legs.

There are two main reasons why epicenter distance is used for determination of the distance between site and source, instead of hypocenter distance. First, for the events with $M_w \leq 6$, the rupture plane is small; hence, epicenter distance and r_{jb} are the same [13]. Here, r_{jb} is the shortest horizontal distance from the recording site to the vertical projection of the rupture plane.

Second, in calculating epicenter distance, it is not necessary to calculate earthquake depth because it may cause error [13].

According to the mentioned notes and the fact that the magnitudes of a vast majority of available

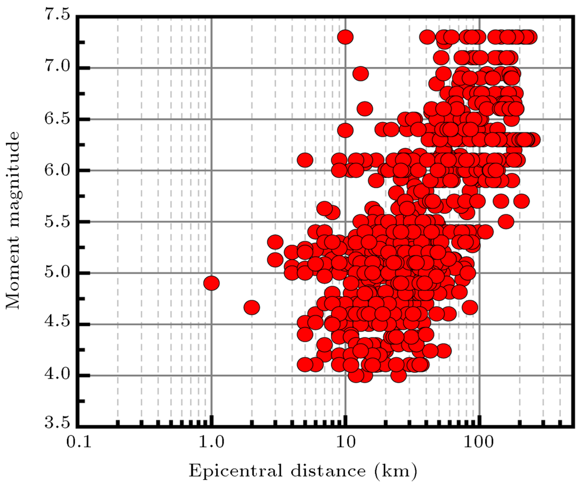

Figure 2. Distribution of the data used in this study in terms of magnitude and distance.

events are less than 6 (see Figure 2), it is advised to use epicenter distance instead of hypocenter distance to measure source-to-site distance. In this paper, three separate attenuation relations are presented for the whole country (Iran), Zagros and Alborz-central Iran zones. Due to underestimation of some regression coefficients, Hypocentral distance is used in two later relations.

As shown in Figure 2, events with magnitudes of 6.5 and over are rarely seen at distances less than 30 Km; hence, the proposed relations must be used with the special consideration at this situation. Figure 3(a) shows the distribution of the selected records as a function of the type of the recording device. It is attempted to select the records that were registered by digital devices with higher quality. Site condition is one of the main factors that affect earthquake parameters and it has significant influence on all important properties of strong ground motion, such as amplitude, frequency content, and duration of ground motion. Influence of site condition on the mentioned parameters depends on geometry, specifications of surface layers materials, site topography, and specifications of input motion. Iran's regulation for

Table 1. Site conditions classification.

Site condition	Type	V_{30}
Rock	1	$V_{30} \geq 750$ m/sec
Stiff soil	2	375 m/sec $\leq V_{30} < 750$ m/sec
Soft soil	3	375 m/sec $> V_{30}$

seismic design of buildings [14] classifies sites into four categories based on average shear velocity measured up to the depth of 30 m (V_{30}).

In order to make the proposed relations consistent with Iran's national regulations for seismic design of buildings [14], conditions of sites are categorized based on average shear velocity measured up to the depth of 30 m [15-18], which is used according to Table 1 (Figure 3(b)).

Many studies have been carried out on Iran's tectonic conditions and its tectonic seismic provinces. One of them is Berberian's study, which divides the Iran zone into 4 large tectonic zones including Zagros, central Iran, Alborz, and Kopehdagh [19]. According to the studies conducted by the second author [7;8], Iran is divided into two main zones: a) Zagros zone and b) Iran without Zagros zone, which is called Alborz-central Iran zone (Figure 3(c)). In the Zagros zone, the frequencies of earthquake occurrence are higher than those in Alborz-central Iran zone, but their magnitudes are lower. Based on the mentioned notes, three separate attenuation relations are presented: (a) a relation for the whole Iran zone, (b) a relation for Zagros zone, and (c) a relation for Alborz-central Iran zone.

In Iran's earthquakes catalogues, the specifications of causative faults have been registered only for a restricted number of records. For this, fault type and other related parameters are not considered in the proposed relations. After analyzing the Iranian strong motion dataset, 806 records from 330 earthquakes were selected.

Boore and Akkar [20] showed that the inelastic response of structures depends on filter frequencies, which are used in processing of strong-motion accelero-

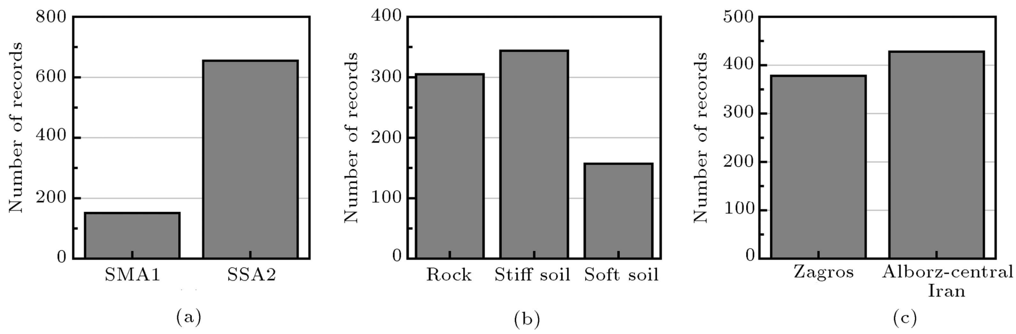

Figure 3. Distribution of the selected records: (a) As a function of the type of the record device, (b) as a function of the site type, and (c) as a function of the tectonic seismic provinces.

grams. Every record has been processed separately, because, unlike acceleration response spectrum, spectral displacement values are very sensitive to filter frequency. In order to process the recorded data, device type should be identified. Iran's earthquakes data have been recorded through two SMA1 and SSA2 devices. The recommended boundaries for correction frequencies were determined according to Ghodrati Amiri et al. [21].

The baseline correction and both high-cut and low-cut filters are used for the correction purpose [22]. Type of the filter is acausal because Boore and Akkar [20] show that the values of inelastic displacement spectrum, which are modified by this filter type, show lower sensitivity to filter frequency. Records were processed by using USPD software [23].

3. Response variable

The main object of this paper is preparation of a Ground Motion Prediction Equation (GMPE) for spectral values of inelastic displacements in Iran zone, since the data of events, which occurred in Iran, are used. Based on the reasons discussed in pervious sections, the calculated inelastic response spectrum is of the constant strength type. For this, inelastic displacement response spectrum was obtained for each earthquake record and strength reduction factors (R) of 1, 2, 4, 6, and 8. According to Figure 1, strength reduction factor (R) is defined as:

$$R = \frac{F_e}{F_y}, \tag{1}$$

where F_e is the elastic strength demand if the system remains elastic and F_y is the yield strength.

Constant strength spectrum for each record and the selected R are computed as follows:

1. Define the ground motion, $\ddot{u}_g(t)$;
2. Select and fix the damping ratio ζ for which the spectrum is to be obtained;
3. Select interested value of period T_n;
4. Determine the response of linear system with T_n and ξ equal to the values selected. The peak elastic force, F_e, is determined from response of linear system;
5. Determine the response (displacement) of an elasto-plastic system with the same T_n and ξ and yield force $F_y = \frac{F_e}{R}$;
6. Repeat steps 1 to 5 for all of the interested periods.

Systems with single degree of freedom have a perfect elastoplastic hysteretic model with viscous damping ratio equal to 5% of critical damping, in which the stiffness and strength degradation in hysteretic behavior are not considered. For each selected record, inelastic displacement spectra are computed at 16 periods ranging from 0.06 to 4 sec. Figure 4 shows an example of constant-strength inelastic displacement response spectrum. Curve fitness process is carried out by using the components which have maximum spectral displacement.

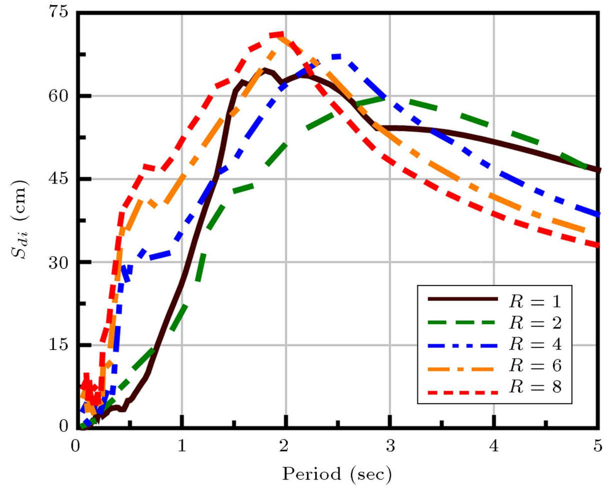

Figure 4. Example of constant-strength inelastic response spectra for the 2003 Bam earthquake, Iran-Bam station.

4. Ground motion prediction equation for inelastic spectral displacement

This paper attempts to present simple relations for inelastic spectral displacement. There are dozens of identified and unidentified parameters affecting strong ground motion. In the proposed relations, it has been tried to consider these parameters based on available data and, regarding the fact that there is limited information about Iran's earthquakes, only the effects of magnitude, distance, and site condition have been taken into account. Also, the influence of tectonic condition is considered by dividing Iran zone into two sub-zones (Zagros and Alborz-central Iran).

4.1. A relation for the whole Iran zone

The format of the ground motion prediction equations is affected by the information recorded in earthquakes catalogues. This means that the accuracy of these relations will be increased by adding more information related to earthquake causative fault and the geometry of rupture plane as well as other effective parameters. Here, due to the shortage of information, the relation has been derived as follows:

$$\log(Y) = a_1 + a_2 M_w + a_3 \left(\log \sqrt{d_{\text{epi}}^2 + a_4^2}\right) + a_5 S_s + a_6 S_A + \varepsilon, \tag{2}$$

in which Y is the earthquake parameter (inelastic

Table 2. The coefficients of Eq. (2). Strength reduction factor is 1.

T (sec)	a_1	a_2	a_3	a_4	a_5	a_6
0.06	-1.926	0.235	-0.981	11.859	-0.016	0.025
0.075	-1.627	0.239	-1.010	11.806	-0.024	0.005
0.1	-1.217	0.242	-1.053	16.207	-0.028	0.028
0.15	-1.249	0.283	-0.958	13.874	0.033	0.084
0.2	-1.261	0.309	-0.893	14.514	0.036	0.079
0.25	-1.318	0.333	-0.866	14.718	0.072	0.102
0.3	-1.356	0.346	-0.833	13.667	0.104	0.099
0.4	-1.609	0.387	-0.765	10.542	0.143	0.111
0.5	-1.871	0.438	-0.723	9.309	0.133	0.092
0.75	-2.372	0.536	-0.690	8.188	0.174	0.075
1	-2.814	0.614	-0.653	6.221	0.179	0.079
1.25	-3.044	0.663	-0.657	6.457	0.201	0.072
1.5	-3.149	0.683	-0.651	6.764	0.208	0.073
2	-3.472	0.737	-0.614	4.969	0.197	0.055
3	-3.698	0.796	-0.612	4.416	0.192	0.066
4	-3.907	0.858	-0.688	4.030	0.198	0.118

spectral displacement); M_w is moment magnitude, d_{epi} is epicenter distance; a_1 to a_6 are regression coefficients (to be computed); and S_s and S_A are site coefficients, which are zero & zero, zero & one, and one & zero, respectively, for rock site, stiff soil site, and soft soil site. Mean terms in Eq. (2) are based on Ambraseys et al. [13]. ε is a random error term with zero mean and standard deviation of σ_T, which is derived from the following equation:

$$\sigma_T = \sqrt{\tau^2 + \sigma^2}. \tag{3}$$

In Eq. (3), τ is the inter-event or between-earthquake standard deviation and σ is the intra-event or within-earthquake standard deviation.

The coefficients of a_1 to a_6 and standard deviations have been calculated for each strength reduction factor and period by using nonlinear mixed-effects regression [24]. Mixed-effects analyses are performed using R software [25]. Tables 2 to 7 show the values of the coefficients introduced in Eqs. (2) and (3).

Computing residual is the best way to investigate efficiency of the proposed relation. According to definition, residual is the difference between observed values and the values predicted by the model. Therefore, positive residual indicates underestimation and negative residual indicates overestimation by our model. Residuals (within group) as a function of distance and magnitude are shown for strength reduction factor, $R = 8$, in Figure 5.

Based on observations, the residuals are not deviated and this proves that the format of the selected relation has covered the effects of distance and magnitude appropriately. In order to further evaluate the proposed model, histograms of the residuals are plotted in Figure 5 for periods of 0.2 sec and 3 sec. Also, the normal distribution fitted to residuals is shown.

In Figure 5, the values in parentheses are mean and standard deviation of the fitted normal distribution. It can be seen that the residuals have a symmetrical bell-shaped histogram, which is evenly distributed around zeros. These indicate that the normality assumption is likely to be true.

Table 3. The coefficients of Eq. (2). Strength reduction factor is 2.

T (sec)	a_1	a_2	a_3	a_4	a_5	a_6
0.06	-3.013	0.398	-0.470	3.871	0.205	0.052
0.075	-2.747	0.361	-0.477	4.055	0.170	0.061
0.1	-2.288	0.325	-0.559	4.597	0.137	0.045
0.15	-1.796	0.315	-0.687	8.326	0.111	0.073
0.2	-1.663	0.332	-0.725	9.201	0.092	0.075
0.25	-1.605	0.349	-0.740	11.086	0.098	0.082
0.3	-1.672	0.359	-0.688	9.297	0.115	0.090
0.4	-1.795	0.422	-0.760	10.610	0.140	0.106
0.5	-1.994	0.457	-0.718	8.941	0.158	0.084
0.75	-2.448	0.548	-0.689	7.793	0.178	0.088
1	-2.790	0.615	-0.677	6.958	0.181	0.077
1.25	-3.013	0.663	-0.686	7.719	0.203	0.078
1.5	-3.141	0.674	-0.640	6.751	0.210	0.082
2	-3.385	0.723	-0.622	5.464	0.193	0.047
3	-3.672	0.797	-0.635	4.797	0.193	0.065
4	-3.815	0.842	-0.691	3.587	0.178	0.108

Table 4. The coefficients of Eq. (2). Strength reduction factor is 4.

T (sec)	a_1	a_2	a_3	a_4	a_5	a_6
0.06	-2.942	0.479	-0.547	4.833	0.210	0.088
0.075	-2.887	0.470	-0.545	5.360	0.213	0.097
0.1	-2.650	0.434	-0.534	4.546	0.207	0.067
0.15	-2.220	0.396	-0.600	6.286	0.196	0.074
0.2	-2.051	0.395	-0.624	7.378	0.151	0.073
0.25	-2.027	0.407	-0.628	6.573	0.152	0.076
0.3	-2.072	0.424	-0.624	6.404	0.125	0.082
0.4	-2.099	0.474	-0.719	10.665	0.173	0.099
0.5	-2.261	0.502	-0.684	8.287	0.178	0.085
0.75	-2.449	0.581	-0.766	13.012	0.169	0.079
1	-2.863	0.623	-0.648	8.826	0.215	0.089
1.25	-3.035	0.665	-0.677	9.405	0.228	0.092
1.5	-3.174	0.686	-0.654	7.469	0.198	0.072
2	-3.459	0.738	-0.636	5.325	0.191	0.059
3	-3.602	0.787	-0.659	4.672	0.221	0.096
4	-3.711	0.826	-0.703	3.859	0.181	0.115

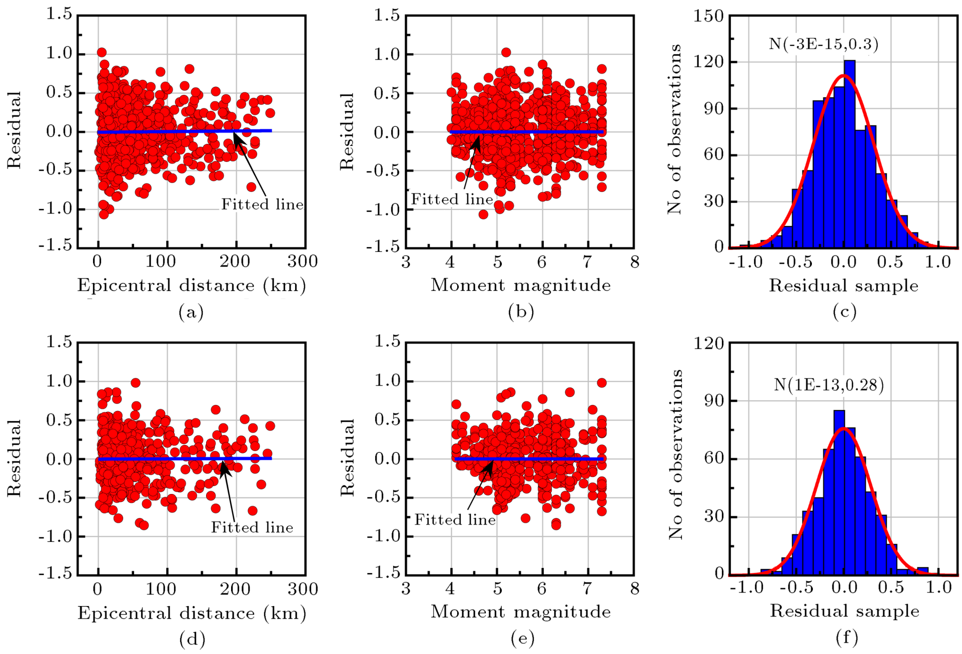

Figure 5. Residuals (within group) as a function of distance and magnitude for strength reduction factor, $R = 8$. Periods are 0.2 sec and 3 sec. Also, histogram of the residuals of the model is plotted. Period of the first row is 0.2 sec and of the second row is 3 sec.

Table 5. The coefficients of Eq. (2). Strength reduction factor is 6.

T (sec)	a_1	a_2	a_3	a_4	a_5	a_6
0.06	-2.861	0.500	-0.605	5.590	0.196	0.100
0.075	-2.803	0.495	-0.607	7.170	0.209	0.104
0.1	-2.687	0.469	-0.565	4.939	0.201	0.081
0.15	-2.391	0.444	-0.589	5.965	0.171	0.054
0.2	-2.260	0.446	-0.627	6.967	0.174	0.076
0.25	-2.275	0.451	-0.595	5.806	0.177	0.078
0.3	-2.236	0.455	-0.597	6.640	0.153	0.078
0.4	-2.250	0.500	-0.697	10.338	0.186	0.102
0.5	-2.403	0.532	-0.682	8.082	0.179	0.083
0.75	-2.621	0.598	-0.723	11.697	0.197	0.088
1	-2.917	0.643	-0.680	9.732	0.236	0.092
1.25	-3.153	0.681	-0.656	8.958	0.220	0.088
1.5	-3.227	0.700	-0.672	7.716	0.205	0.085
2	-3.481	0.744	-0.647	5.176	0.204	0.075
3	-3.598	0.794	-0.684	5.309	0.202	0.089
4	-3.789	0.835	-0.690	3.992	0.188	0.107

Table 6. The coefficients of Eq. (2). Strength reduction factor is 8.

T (sec)	a_1	a_2	a_3	a_4	a_5	a_6
0.06	-2.800	0.504	-0.628	6.247	0.185	0.103
0.075	-2.771	0.504	-0.624	7.538	0.192	0.103
0.1	-2.717	0.493	-0.590	5.665	0.197	0.090
0.15	-2.488	0.480	-0.617	7.173	0.161	0.055
0.2	-2.383	0.477	-0.628	7.018	0.185	0.076
0.25	-2.416	0.485	-0.605	6.203	0.177	0.083
0.3	-2.350	0.487	-0.614	7.486	0.162	0.074
0.4	-2.380	0.526	-0.695	9.849	0.189	0.099
0.5	-2.451	0.556	-0.717	10.379	0.182	0.077
0.75	-2.688	0.613	-0.731	11.522	0.204	0.086
1	-2.973	0.664	-0.713	10.210	0.225	0.089
1.25	-3.161	0.687	-0.673	8.838	0.221	0.090
1.5	-3.252	0.709	-0.687	7.937	0.213	0.075
2	-3.509	0.748	-0.646	5.164	0.207	0.075
3	-3.575	0.793	-0.703	5.779	0.201	0.089
4	-3.807	0.837	-0.696	4.132	0.195	0.114

4.2. A relation for Zagros zone

Due to limited information in this zone, the mathematical format of the Zagros zone relation has been selected as follows:

$$\log(Y) = a_1 + a_2 M_w + a_3 \left(\log\sqrt{d_{\text{epi}}^2 + h_{\text{hypo}}^2}\right) + a_4 S_s + \varepsilon, \tag{4}$$

in which Y is earthquake parameter (inelastic displacement), M_w is moment magnitude, d_{epi} is epicentral distance, h_{hypo} is focal depth, and a_1 to a_4 are regression coefficients (should be calculated). S_s is site factor, which is zero for rock site condition and one for stiff and soft soil conditions. The other terms are already defined.

Eq. (4) differs from Eq. (2). The term $\log\left(\sqrt{d_{\text{epi}}^2 + h_{\text{hypo}}^2}\right)$ (hypocentral distance) is replaced by $\log\left(\sqrt{d_{\text{epi}}^2 + a_5^2}\right)$. The reason for this substitution

Table 7. The standard deviations of Eq. (2) versus strength reduction factor values.

R	1	1	1	2	2	2	4	4	4	6	6	6	8	8	8
T (sec)	τ	σ	σ_T	τ	σ	σ_T	τ	σ	σ_T	τ	σ	σ_T	τ	σ	σ_T
0.06	0.13	0.30	0.33	0.14	0.37	0.40	0.15	0.37	0.40	0.14	0.36	0.39	0.14	0.35	0.38
0.075	0.13	0.30	0.32	0.12	0.37	0.39	0.16	0.37	0.40	0.14	0.37	0.39	0.14	0.36	0.38
0.1	0.11	0.31	0.32	0.12	0.34	0.36	0.13	0.37	0.40	0.14	0.37	0.39	0.14	0.36	0.38
0.15	0.11	0.30	0.32	0.12	0.30	0.33	0.13	0.34	0.36	0.13	0.35	0.37	0.13	0.36	0.38
0.2	0.10	0.31	0.32	0.12	0.30	0.32	0.13	0.32	0.35	0.15	0.33	0.36	0.14	0.34	0.37
0.25	0.10	0.31	0.32	0.12	0.30	0.33	0.14	0.33	0.35	0.14	0.34	0.37	0.15	0.34	0.37
0.3	0.13	0.31	0.34	0.14	0.30	0.33	0.14	0.32	0.35	0.14	0.34	0.37	0.15	0.34	0.37
0.4	0.18	0.31	0.36	0.17	0.30	0.35	0.15	0.32	0.35	0.16	0.34	0.37	0.16	0.34	0.38
0.5	0.19	0.30	0.36	0.18	0.31	0.36	0.17	0.32	0.37	0.18	0.33	0.38	0.18	0.33	0.38
0.75	0.21	0.32	0.38	0.20	0.31	0.37	0.19	0.32	0.37	0.19	0.33	0.38	0.20	0.33	0.39
1	0.22	0.32	0.39	0.21	0.32	0.38	0.20	0.32	0.38	0.22	0.32	0.39	0.22	0.33	0.39
1.25	0.24	0.32	0.40	0.23	0.32	0.39	0.23	0.32	0.40	0.23	0.33	0.40	0.23	0.33	0.41
1.5	0.24	0.34	0.41	0.24	0.32	0.40	0.25	0.33	0.41	0.26	0.33	0.42	0.25	0.33	0.42
2	0.25	0.33	0.41	0.24	0.33	0.40	0.23	0.34	0.41	0.24	0.34	0.41	0.24	0.34	0.42
3	0.22	0.31	0.38	0.21	0.31	0.37	0.22	0.30	0.37	0.21	0.32	0.38	0.21	0.32	0.38
4	0.21	0.31	0.38	0.21	0.30	0.37	0.19	0.31	0.37	0.18	0.32	0.37	0.17	0.32	0.36

Table 8. The coefficients of Eq. (4) for Zagros zone. Strength reduction factor is 1.

T (sec)	a_1	a_2	a_3	a_4
0.06	-1.939	0.161	-0.646	-0.024
0.075	-1.709	0.175	-0.663	-0.041
0.1	-1.396	0.165	-0.626	-0.016
0.15	-1.476	0.269	-0.705	0.032
0.2	-1.502	0.305	-0.672	0.016
0.25	-1.659	0.348	-0.646	0.049
0.3	-1.732	0.369	-0.616	0.046
0.4	-1.839	0.418	-0.652	0.063
0.5	-1.955	0.461	-0.674	0.045
0.75	-2.447	0.573	-0.692	0.056
1	-2.834	0.667	-0.749	0.080
1.25	-3.074	0.727	-0.791	0.088
1.5	-3.068	0.733	-0.818	0.096
2	-3.255	0.766	-0.803	0.078
3	-3.303	0.785	-0.785	0.073
4	-3.371	0.820	-0.846	0.108

Table 9. The coefficients of Eq. (4) for Zagros zone. Strength reduction factor is 2.

T (sec)	a_1	a_2	a_3	a_4
0.06	-3.043	0.473	-0.660	0.039
0.075	-2.735	0.414	-0.607	0.021
0.1	-2.095	0.323	-0.613	0.022
0.15	-1.814	0.323	-0.637	0.051
0.2	-1.765	0.343	-0.628	0.026
0.25	-1.856	0.381	-0.624	0.032
0.3	-1.854	0.391	-0.614	0.041
0.4	-1.990	0.456	-0.680	0.054
0.5	-2.076	0.490	-0.699	0.041
0.75	-2.420	0.571	-0.709	0.065
1	-2.779	0.660	-0.765	0.080
1.25	-3.003	0.712	-0.801	0.097
1.5	-3.027	0.720	-0.811	0.095
2	-3.150	0.751	-0.822	0.076
3	-3.331	0.789	-0.778	0.063
4	-3.295	0.813	-0.874	0.106

is the fact that the estimated value of the coefficient of a_5 was low. The second difference of Eq. (3) is the deletion of S_A and considering both site types 2 and 3 as a group, i.e. soil site. Because numbers of available records are low in this region, both site types 2 and 3 are considered within one group of site conditions. Regression coefficient and standard deviation of Eq. (4) for each selected strength reduction factor are shown in Tables 8 to 13.

4.3. A relation for Alborz-central Iran zone

The mathematical form of the selected relation is as follows:

$$\log(Y) = a_1 + a_2 M_w + a_3 \left(\log\sqrt{d_{\text{epi}}^2 + h_{\text{hypo}}^2}\right) + a_4 S_s + a_5 S_A + \varepsilon, \qquad (5)$$

in which Y is earthquake parameter (inelastic displace-

Table 10. The coefficients of Eq. (4) for Zagros zone. Strength reduction factor is 4.

T (sec)	a_1	a_2	a_3	a_4
0.06	-3.012	0.556	-0.706	0.056
0.075	-2.862	0.532	-0.718	0.064
0.1	-2.615	0.493	-0.699	0.045
0.15	-2.275	0.438	-0.636	0.045
0.2	-2.187	0.441	-0.626	0.046
0.25	-2.094	0.445	-0.641	0.035
0.3	-2.043	0.460	-0.691	0.034
0.4	-2.238	0.488	-0.615	0.063
0.5	-2.318	0.533	-0.682	0.062
0.75	-2.527	0.596	-0.719	0.070
1	-2.834	0.651	-0.707	0.108
1.25	-3.026	0.704	-0.759	0.112
1.5	-3.049	0.728	-0.821	0.080
2	-3.268	0.777	-0.833	0.071
3	-3.206	0.774	-0.813	0.076
4	-3.095	0.779	-0.881	0.084

Table 11. The coefficients of Eq. (4) for Zagros zone. Strength reduction factor is 6.

T (sec)	a_1	a_2	a_3	a_4
0.06	-2.846	0.539	-0.686	0.074
0.075	-2.789	0.535	-0.700	0.082
0.1	-2.622	0.501	-0.657	0.060
0.15	-2.392	0.479	-0.642	0.027
0.2	-2.319	0.480	-0.638	0.060
0.25	-2.207	0.485	-0.693	0.062
0.3	-2.179	0.487	-0.672	0.036
0.4	-2.347	0.511	-0.609	0.072
0.5	-2.362	0.555	-0.718	0.059
0.75	-2.648	0.621	-0.731	0.079
1	-2.905	0.671	-0.731	0.113
1.25	-3.107	0.713	-0.741	0.112
1.5	-3.084	0.737	-0.832	0.094
2	-3.247	0.773	-0.838	0.080
3	-3.228	0.782	-0.824	0.057
4	-3.134	0.768	-0.825	0.092

ment), M_w is moment magnitude, d_{epi} is epicentral distance, h_{hypo} is focal depth, and a_1 to a_5 are regression coefficients (to be calculated). S_s and S_A are site factors, which are zero & zero, zero & one, and one & zero for site conditions 1, 2, and 3, respectively. Tables 14 to 19 show the coefficients and standard deviations of Eq. (5).

Table 12. The coefficients of Eq. (4) for Zagros zone. Strength reduction factor is 8.

T (sec)	a_1	a_2	a_3	a_4
0.06	-2.773	0.531	-0.675	0.077
0.075	-2.731	0.529	-0.678	0.082
0.1	-2.668	0.518	-0.648	0.071
0.15	-2.489	0.501	-0.632	0.035
0.2	-2.381	0.503	-0.658	0.071
0.25	-2.283	0.507	-0.707	0.075
0.3	-2.322	0.505	-0.631	0.050
0.4	-2.374	0.529	-0.650	0.076
0.5	-2.440	0.566	-0.695	0.058
0.75	-2.686	0.629	-0.738	0.087
1	-2.980	0.687	-0.732	0.107
1.25	-3.076	0.711	-0.754	0.113
1.5	-3.045	0.724	-0.818	0.094
2	-3.229	0.773	-0.850	0.082
3	-3.184	0.771	-0.824	0.068
4	-3.173	0.771	-0.819	0.101

5. A numerical example of the ground motion prediction equation for inelastic displacement

Figure 6 shows the decay of estimated inelastic spectral displacement at 0.06 sec and 1 sec of natural period with distance for M_w = 5.5, 6, 6.5, and 7 at a rock site condition in Iran. This figure shows decay rate for short and long periods.

Figure 7 shows the effects of local site condition on inelastic spectral displacement in Iran zone for an event with moment magnitude of 6.5. Strength reduction factors are equal to 4 and 8 and sites are located at 20 km and 50 km from source. This figure shows that site condition has significant effects on inelastic spectral displacement and, as expected, the values of displacement for soft soil site condition are higher than those for the other sites.

Also, Figure 8 shows the effect of strength reduction factor on inelastic spectral displacement. As shown in Figure 8, by increasing the strength reduction in low periods range, the inelastic displacements increased. In contrast, in the range of long periods, by increasing the strength reduction factor, the values of inelastic displacement decreased.

Figure 9 shows the effects of local site condition on inelastic spectral displacement for an event with moment magnitude of 6 in Zagros zone. Figure 10 shows distance attenuation of the estimated inelastic spectral displacement at a soil site condition for a period of 0.5 sec and strength reductions of 4 and 8 in Zagros zone.

Table 13. The standard deviations of Eq. (4) versus strength reduction factor values.

R	1	1	1	2	2	2	4	4	4	6	6	6	8	8	8
T (sec)	τ	σ	σ_T	τ	σ	σ_T	τ	σ	σ_T	τ	σ	σ_T	τ	σ	σ_T
0.06	0.11	0.36	0.37	0.07	0.39	0.40	0.0001	0.41	0.41	0.00008	0.41	0.41	0.046	0.39	0.39
0.075	0.12	0.35	0.37	0.04	0.39	0.39	0.0402	0.42	0.42	0.00037	0.41	0.41	0.050	0.40	0.40
0.1	0.10	0.35	0.36	0.04	0.37	0.37	0.0000	0.41	0.41	0.00004	0.41	0.41	0.017	0.40	0.40
0.15	0.13	0.34	0.36	0.06	0.35	0.35	0.0000	0.37	0.37	0.00003	0.38	0.38	0.000	0.39	0.39
0.2	0.08	0.36	0.37	0.00	0.35	0.35	0.0000	0.36	0.36	0.04503	0.37	0.38	0.040	0.37	0.38
0.25	0.09	0.35	0.36	0.00	0.36	0.36	0.0356	0.37	0.38	0.09603	0.37	0.38	0.072	0.37	0.38
0.3	0.00	0.38	0.38	0.06	0.36	0.36	0.0284	0.37	0.37	0.00004	0.38	0.38	0.000	0.37	0.37
0.4	0.12	0.36	0.38	0.10	0.36	0.37	0.0584	0.36	0.37	0.08049	0.37	0.38	0.107	0.37	0.38
0.5	0.15	0.34	0.37	0.13	0.34	0.37	0.1167	0.35	0.37	0.13802	0.34	0.37	0.135	0.35	0.37
0.75	0.12	0.37	0.39	0.12	0.36	0.38	0.1466	0.35	0.38	0.16665	0.35	0.38	0.175	0.35	0.39
1	0.14	0.37	0.39	0.15	0.35	0.38	0.1528	0.35	0.38	0.19002	0.34	0.39	0.185	0.34	0.39
1.25	0.20	0.35	0.40	0.19	0.35	0.40	0.2079	0.34	0.40	0.20560	0.34	0.40	0.206	0.34	0.40
1.5	0.22	0.35	0.41	0.22	0.34	0.40	0.2383	0.33	0.41	0.24447	0.33	0.41	0.234	0.34	0.41
2	0.23	0.35	0.42	0.21	0.35	0.41	0.2027	0.35	0.40	0.20782	0.35	0.41	0.224	0.35	0.41
3	0.22	0.31	0.38	0.18	0.33	0.37	0.1955	0.32	0.37	0.20704	0.31	0.38	0.215	0.31	0.38
4	0.16	0.34	0.38	0.14	0.35	0.38	0.1445	0.35	0.37	0.11470	0.36	0.37	0.109	0.36	0.37

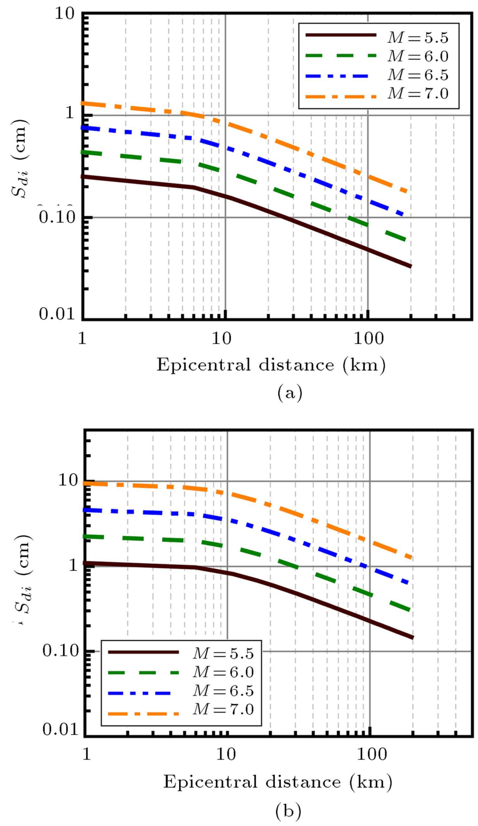

Figure 6. Decay of the estimated inelastic spectral displacement at (a) 0.06 sec and (b) 1 sec of natural period with distance for M_w = 5.5, 6, 6.5, and 7 at a rock site condition in Iran. Strength reduction factor is equal to 4.

Table 14. The coefficients of Eq. (5). Strength reduction factor is 1.

T (sec)	a_1	a_2	a_3	a_4	a_5
0.06	-1.613	0.210	-1.064	0.048	0.046
0.075	-1.304	0.209	-1.086	0.029	0.030
0.1	-1.145	0.231	-1.060	0.022	0.054
0.15	-0.996	0.240	-0.954	0.087	0.118
0.2	-1.046	0.259	-0.851	0.115	0.116
0.25	-1.076	0.283	-0.835	0.156	0.121
0.3	-1.023	0.289	-0.823	0.191	0.100
0.4	-1.173	0.332	-0.820	0.241	0.119
0.5	-1.438	0.397	-0.825	0.234	0.117
0.75	-1.909	0.493	-0.799	0.273	0.090
1	-2.276	0.564	-0.774	0.260	0.084
1.25	-2.480	0.604	-0.759	0.278	0.066
1.5	-2.609	0.632	-0.760	0.282	0.061
2	-2.879	0.688	-0.742	0.248	0.046
3	-3.146	0.757	-0.762	0.258	0.070
4	-3.357	0.825	-0.854	0.240	0.135

Figure 11 represented inelastic spectral displacement for an event with moment magnitude of 6.5 in Alborz-central Iran zone. Strength reduction factors are equal to 4 and 8. Sites are located at 20 km and 50 km from source. Figure 12 shows distance attenuation of the estimated inelastic spectral displacement at

Table 15. The coefficients of Eq. (5). Strength reduction factor is 2.

T (sec)	a_1	a_2	a_3	a_4	a_5
0.06	-2.507	0.331	-0.511	0.294	0.052
0.075	-2.329	0.296	-0.492	0.276	0.089
0.1	-1.955	0.274	-0.565	0.218	0.059
0.15	-1.420	0.265	-0.718	0.173	0.076
0.2	-1.259	0.277	-0.759	0.175	0.091
0.25	-1.212	0.284	-0.742	0.188	0.094
0.3	-1.238	0.303	-0.736	0.199	0.099
0.4	-1.377	0.364	-0.799	0.245	0.123
0.5	-1.545	0.409	-0.810	0.270	0.113
0.75	-2.022	0.511	-0.801	0.282	0.108
1	-2.287	0.570	-0.793	0.270	0.077
1.25	-2.508	0.614	-0.785	0.280	0.066
1.5	-2.618	0.629	-0.760	0.287	0.083
2	-2.820	0.674	-0.738	0.247	0.036
3	-3.114	0.760	-0.798	0.266	0.087
4	-3.240	0.801	-0.844	0.215	0.113

Table 16. The coefficients of Eq. (5). Strength reduction factor is 4.

T (sec)	a_1	a_2	a_3	a_4	a_5
0.06	-2.360	0.411	-0.630	0.325	0.092
0.075	-2.357	0.406	-0.611	0.333	0.098
0.1	-2.146	0.359	-0.551	0.321	0.070
0.15	-1.801	0.341	-0.648	0.304	0.089
0.2	-1.595	0.336	-0.671	0.245	0.070
0.25	-1.564	0.351	-0.696	0.264	0.089
0.3	-1.666	0.375	-0.683	0.241	0.101
0.4	-1.718	0.436	-0.798	0.268	0.106
0.5	-1.790	0.463	-0.814	0.288	0.090
0.75	-2.155	0.547	-0.811	0.265	0.082
1	-2.470	0.589	-0.735	0.285	0.074
1.25	-2.621	0.629	-0.773	0.296	0.087
1.5	-2.669	0.646	-0.780	0.283	0.075
2	-2.883	0.690	-0.771	0.263	0.062
3	-3.036	0.751	-0.832	0.313	0.127
4	-3.147	0.790	-0.871	0.240	0.146

a site with stiff soil condition for a period of 0.5 sec and strength reductions of 4 and 8 in Alborz-central Iran zone.

6. Comparison

There are a few GMPEs for constant-strength inelastic spectral displacement. Tothong and Cornell [2] proposed a GMPE for inelastic spectral displacement as a function of moment magnitude and predicted median strength reduction factor (R). The model proposed by Tothong and Cornell [2] is expressed in following

Table 17. The coefficients of Eq. (5). Strength reduction factor is 6.

T (sec)	a_1	a_2	a_3	a_4	a_5
0.06	-2.299	0.447	-0.723	0.290	0.099
0.075	-2.277	0.444	-0.709	0.308	0.100
0.1	-2.168	0.410	-0.647	0.309	0.079
0.15	-1.944	0.398	-0.679	0.284	0.064
0.2	-1.811	0.397	-0.699	0.268	0.069
0.25	-1.828	0.402	-0.673	0.283	0.076
0.3	-1.840	0.413	-0.683	0.266	0.109
0.4	-1.879	0.466	-0.785	0.290	0.107
0.5	-1.955	0.496	-0.805	0.292	0.096
0.75	-2.295	0.565	-0.787	0.291	0.096
1	-2.523	0.610	-0.775	0.301	0.086
1.25	-2.721	0.651	-0.775	0.284	0.077
1.5	-2.737	0.662	-0.800	0.292	0.085
2	-2.905	0.700	-0.797	0.279	0.089
3	-3.050	0.755	-0.846	0.301	0.124
4	-3.284	0.810	-0.858	0.236	0.131

Table 18. The coefficients of Eq. (5). Strength reduction factor is 8.

T (sec)	a_1	a_2	a_3	a_4	a_5
0.06	-2.264	0.461	-0.767	0.279	0.105
0.075	-2.278	0.463	-0.745	0.283	0.102
0.1	-2.187	0.444	-0.712	0.300	0.087
0.15	-2.006	0.441	-0.741	0.267	0.048
0.2	-1.929	0.431	-0.710	0.271	0.061
0.25	-1.980	0.445	-0.697	0.271	0.076
0.3	-1.923	0.454	-0.738	0.260	0.085
0.4	-1.991	0.494	-0.796	0.296	0.103
0.5	-2.066	0.528	-0.833	0.292	0.090
0.75	-2.359	0.579	-0.789	0.288	0.084
1	-2.567	0.634	-0.822	0.288	0.085
1.25	-2.729	0.662	-0.810	0.291	0.078
1.5	-2.778	0.681	-0.833	0.296	0.065
2	-2.963	0.706	-0.782	0.280	0.084
3	-3.036	0.759	-0.869	0.289	0.112
4	-3.314	0.811	-0.856	0.239	0.137

equations:

$$\ln \frac{S_{di}}{S_{de}}; \qquad R \leq 0.2,$$

$$\begin{aligned} \ln \frac{S_{di}}{S_{de}} &= g_1(R, M_w) + g_2(R). (M_w - 6.5) \\ &\quad - g_1(0.2, M_w) + \varepsilon_{\ln(S_{di}/S_{de})}, \\ &\quad 0.2 \leq R \leq 10, \end{aligned} \tag{6}$$

where:

Table 19. The standard deviations of Eq. (5) versus strength reduction factor values.

R	1	1	1	2	2	2	4	4	4	6	6	6	8	8	8
T(sec)	τ	σ	σ_T	τ	σ	σ_T	τ	σ	σ_T	τ	σ	σ_T	τ	σ	σ_T
0.06	0.18	0.26	0.32	0.14	0.36	0.38	0.17	0.33	0.37	0.17	0.32	0.37	0.16	0.32	0.36
0.075	0.18	0.26	0.32	0.14	0.35	0.38	0.18	0.33	0.38	0.16	0.33	0.37	0.16	0.33	0.37
0.1	0.14	0.28	0.31	0.14	0.33	0.36	0.16	0.35	0.38	0.18	0.33	0.38	0.17	0.33	0.37
0.15	0.11	0.28	0.30	0.12	0.29	0.31	0.14	0.32	0.35	0.15	0.33	0.36	0.15	0.33	0.36
0.2	0.09	0.28	0.29	0.12	0.26	0.29	0.14	0.31	0.34	0.15	0.31	0.35	0.16	0.32	0.35
0.25	0.07	0.28	0.29	0.12	0.27	0.30	0.14	0.30	0.33	0.15	0.31	0.35	0.16	0.32	0.36
0.3	0.11	0.28	0.30	0.13	0.27	0.30	0.15	0.30	0.33	0.17	0.31	0.35	0.18	0.32	0.37
0.4	0.17	0.28	0.33	0.17	0.27	0.32	0.17	0.30	0.34	0.18	0.32	0.36	0.19	0.33	0.37
0.5	0.19	0.28	0.34	0.19	0.28	0.34	0.19	0.31	0.36	0.19	0.31	0.37	0.19	0.32	0.37
0.75	0.22	0.29	0.36	0.22	0.29	0.36	0.20	0.30	0.36	0.20	0.31	0.37	0.20	0.32	0.38
1	0.22	0.30	0.37	0.22	0.30	0.37	0.20	0.30	0.36	0.22	0.31	0.38	0.23	0.32	0.39
1.25	0.23	0.30	0.38	0.21	0.31	0.38	0.22	0.31	0.39	0.23	0.32	0.39	0.24	0.32	0.40
1.5	0.22	0.32	0.39	0.22	0.31	0.39	0.23	0.32	0.40	0.25	0.32	0.40	0.25	0.32	0.41
2	0.23	0.32	0.39	0.24	0.31	0.39	0.23	0.33	0.40	0.25	0.32	0.41	0.24	0.33	0.41
3	0.21	0.31	0.37	0.22	0.30	0.37	0.22	0.30	0.37	0.22	0.32	0.38	0.21	0.32	0.38
4	0.22	0.30	0.37	0.21	0.29	0.36	0.19	0.30	0.35	0.19	0.31	0.36	0.19	0.31	0.36

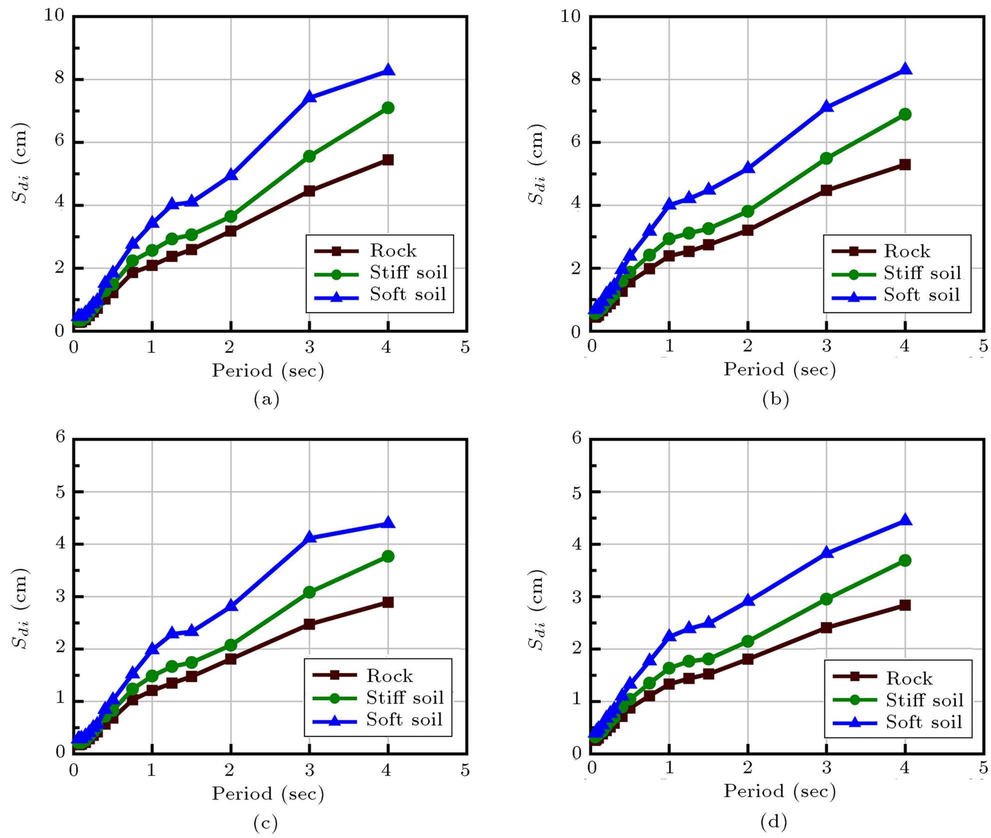

Figure 7. Effects of local site condition on inelastic spectral displacement in Iran region for an event with moment magnitude of 6.5. The first rows in graphs are for the site located at 20 km and the second rows are for the site located at 50 km. Strength reduction factor for left-column graphs is equal to 4. Strength reduction factor for right-column graphs is equal to 8.

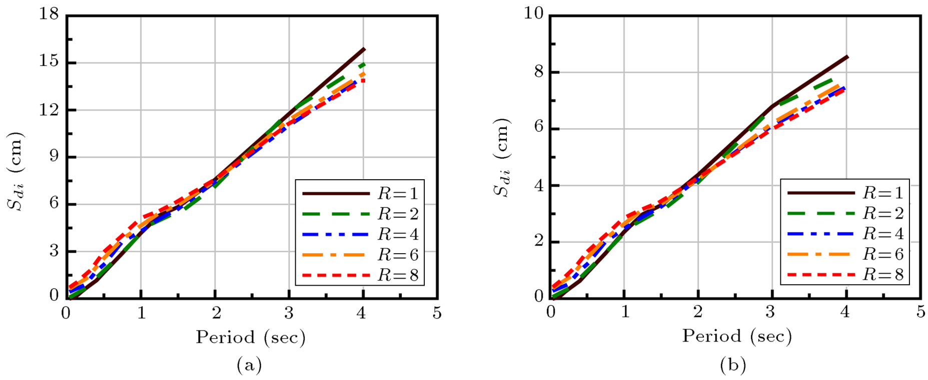

Figure 8. Effect of strength reduction factor (R) on inelastic spectral displacement: (a) Site to source distance is equal to 20 km; rock site, $M_w = 7$, and (b) site to source distance is equal to 50 km; rock site, $M_w = 7$.

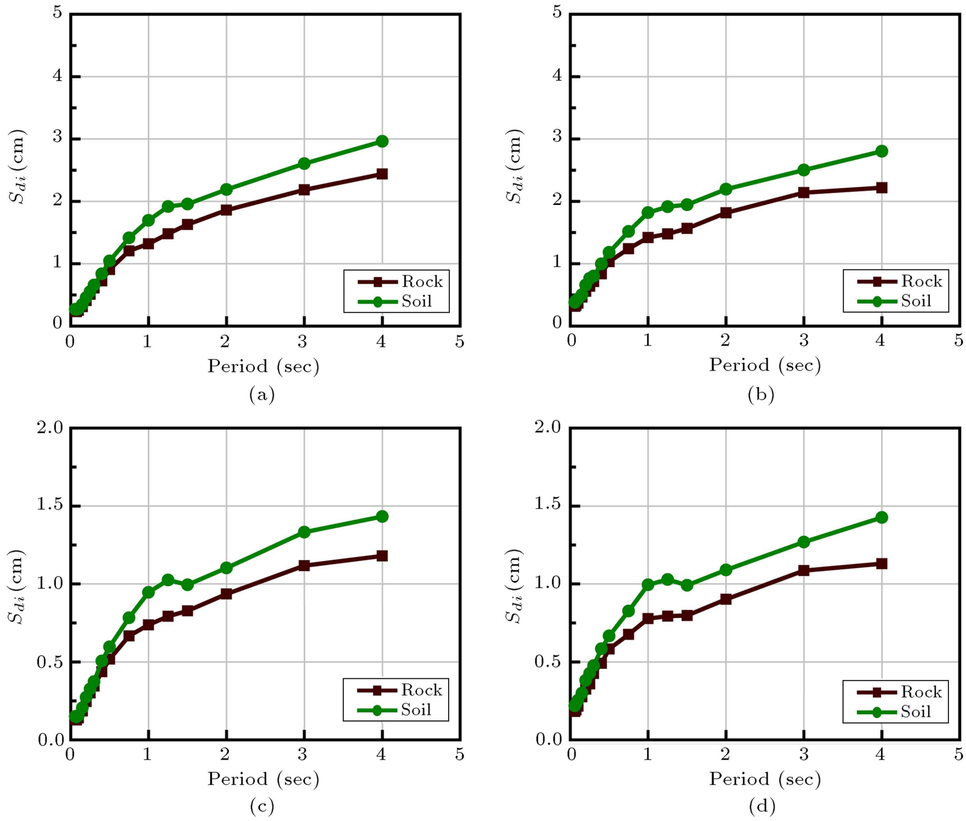

Figure 9. Effects of local site condition on inelastic spectral displacement in Zagros region for an event with moment magnitude of 6. The first rows in graphs are for the site located at 20 km and the second rows are for site located at 50 km. Strength reduction factor for left-column graphs is equal to 4. Strength reduction factor for right-column graphs is equal to 8. Focal depth is equal to 10 km.

$$g_1(R, M_w) = (\beta_1 + \beta_2 M_w)R + (\beta_3 + \beta_4 M_w)R.\ln(R) + \beta_5.R^{2.5}, \tag{7}$$

$$g_2(R) = \begin{cases} 0 & R \leq 0.3 \\ 0.37(\beta_6)(R - 0.3) & 0.3 \leq R \leq 3 \\ \beta_6 & 3 \leq R \leq 10 \end{cases} \tag{8}$$

In Eqs. (6)-(8), β_1 through β_6 and $\varepsilon_{\ln(S_{di}/S_{de})}$ are the regression parameters. Once $\ln \frac{S_{di}}{S_{de}}$ is computed, it is multiplied by S_{de} (elastic displacement) to obtain S_{di} (inelastic displacement). The elastic displacement S_{de} can be computed from elastic GMPE.

For comparison, Tothong and Cornell [2] model is used with other elastic GMPEs, such as Campbell and Bozorgnia [26], Boore and Atkinson [27], Ambraseys et al. [13], Ghodrati Amiri et al. [8], Ghasemi et al. [28], Saffari et al. [29], and Hassani et al. [30]. Elastic GMPEs are used to obtain elastic displacement. These elastic GMPEs are classified in two categories. The

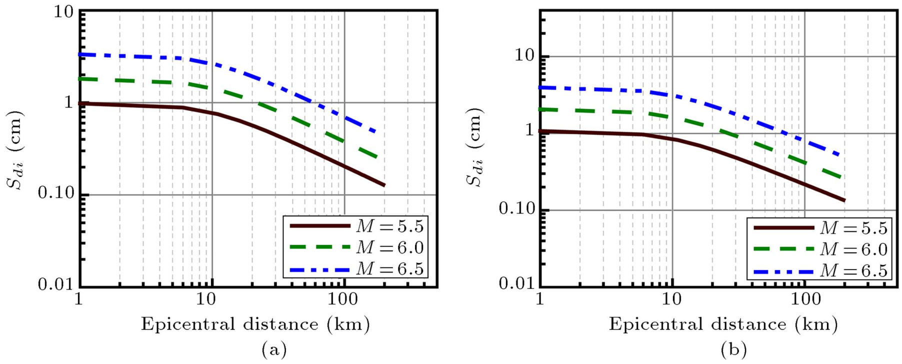

Figure 10. Distance attenuation of estimated inelastic spectral displacement at a site with soil in Zagros region for a period of 0.5 sec. Strength reduction factors are equal to (a) 4 and (b) 8. Focal depth is equal to 10 km.

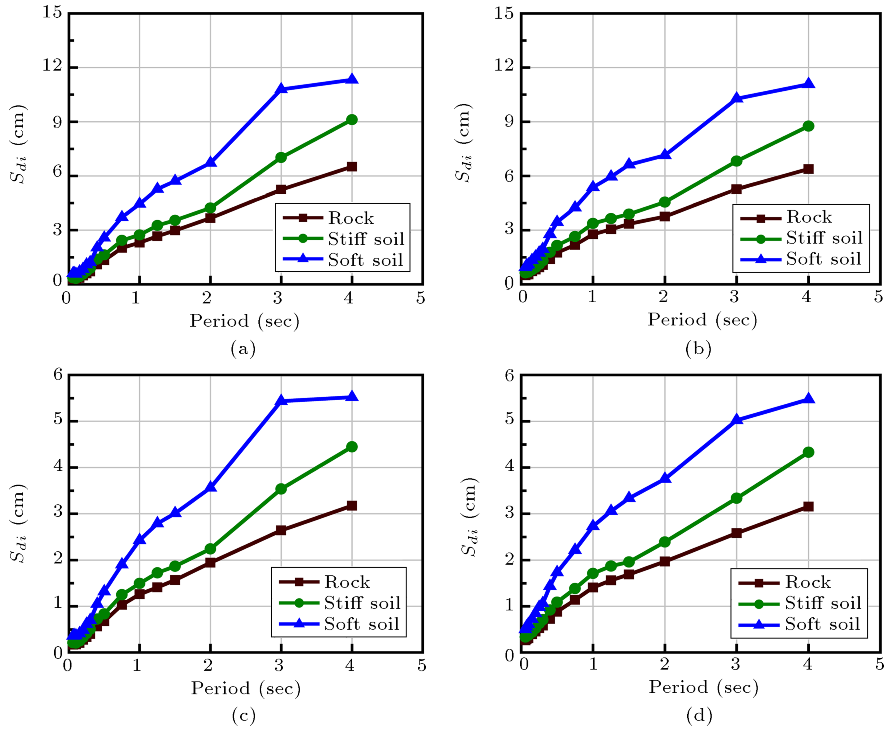

Figure 11. Effects of local site condition on inelastic spectral displacement in Alborz-central Iran region for an event with moment magnitude of 6.5. The first rows in graphs are for the site located at 20 km and the second rows are for the site located at 50 km. Strength reduction factor for left-column graphs is equal to 4. Strength reduction factor for right-column graphs is equal to 8. Focal depth is equal 10 km.

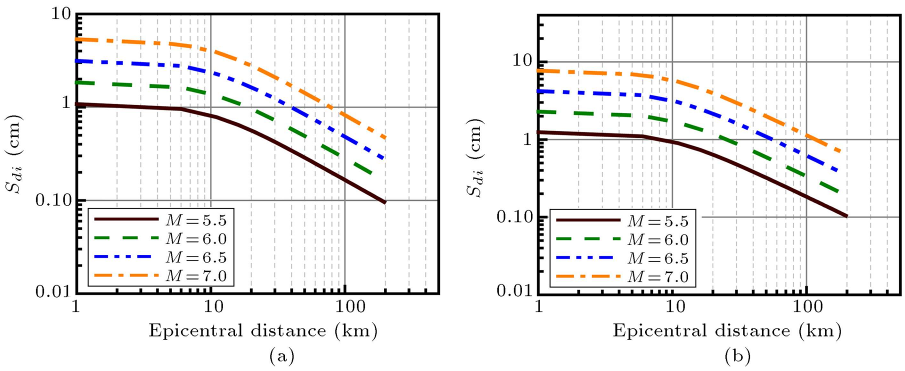

Figure 12. Distance attenuation of the estimated inelastic spectral displacement at a site with stiff soil in Alborz-central Iran region for the period of 0.5 sec. Strength reduction factors equal: (a) 4 and (b) 8. Focal depth is equal to 10 km.

first group includes equations that were obtained based on Iran earthquakes [8,28-30]. In the second group, equations were obtained using some of the events that occurred in Iran [13,26,27]. Also, Shoja-Taheri et al. [31] showed the two NGA models of Boore and Atkinson [27] and Campbell and Bozorgnia [26] had good agreement with Iranian dataset.

The results of comparison between the equation proposed in this study for Iran zone and the equation proposed by Tothong and Cornell [2] are shown in Figure 13. In Figure 13, strength reduction factor is equal to 4. As can be seen, in rock and stiff soil sites in the range of long periods, the estimated inelastic displacement from the equation proposed in this study is larger than those from other equations. From results of comparison, it could be concluded that the Boore and Atkinson model [27] is appropriate to estimate inelastic displacement by using Tothong and Cornell [2] model in soft soil sites. But, the model proposed by Campbell and Bozorgnia [26] overestimates the inelastic displacement in near-fault region for soft soil sites.

The results of comparison between the equations proposed in this study for Alborz-central Iran and

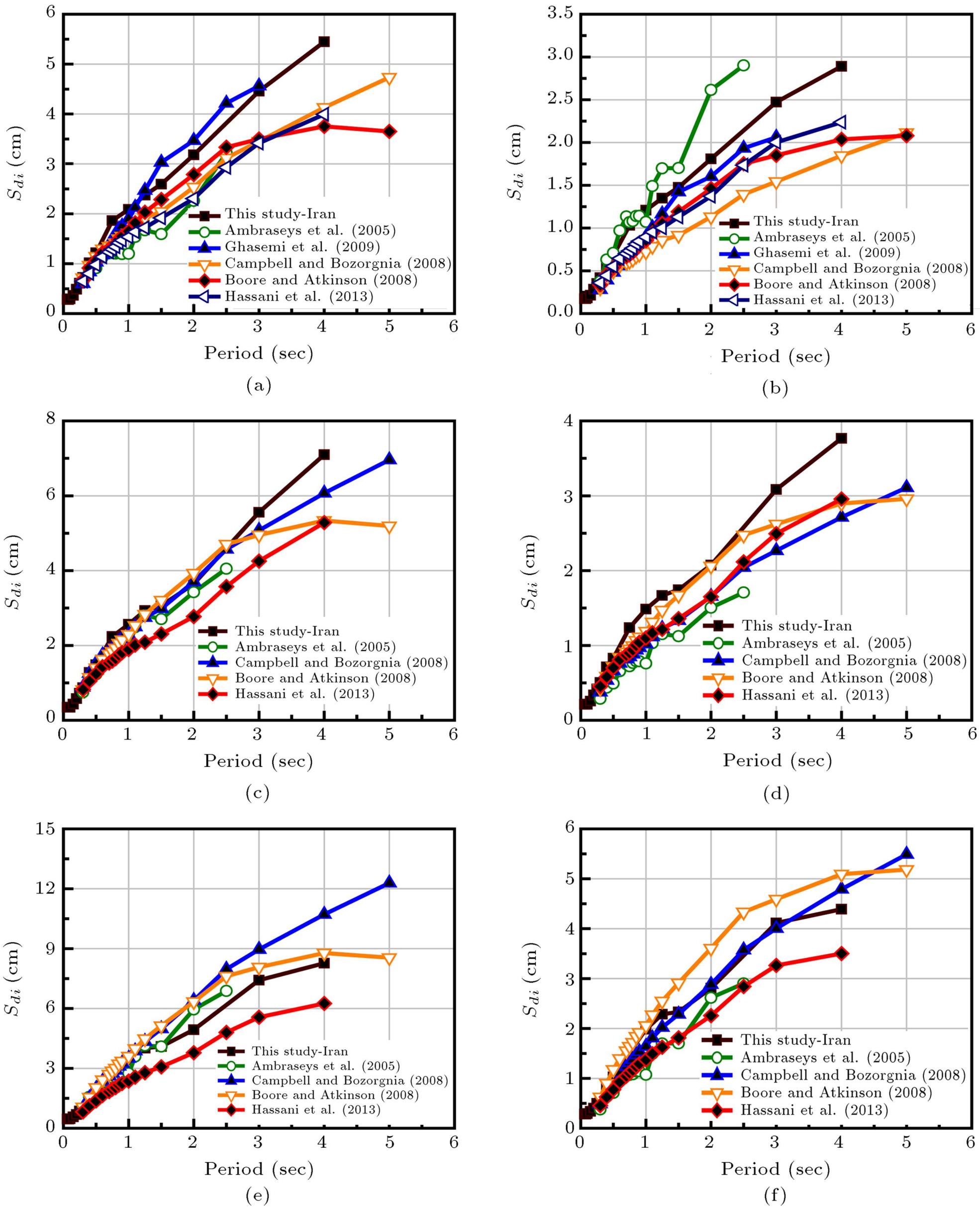

Figure 13. Comparison between equations proposed in this study for Iran region and the equation proposed by Tothong and Cornell [2]. The elastic displacement is obtained from various elastic GMPEs (shown in graph). Left-column graphs are for $M_w = 6.5$ and distance of 20 km. Right-column graphs are for $M_w = 6.5$ and distance of 50 km. In (a) and (b) $V_{30} = 800$ m/sec; in (c) and (d) $V_{30} = 500$ m/sec; and in (e) and (f) $V_{30} = 250$ m/sec. Strength reduction factor is equal to 4.

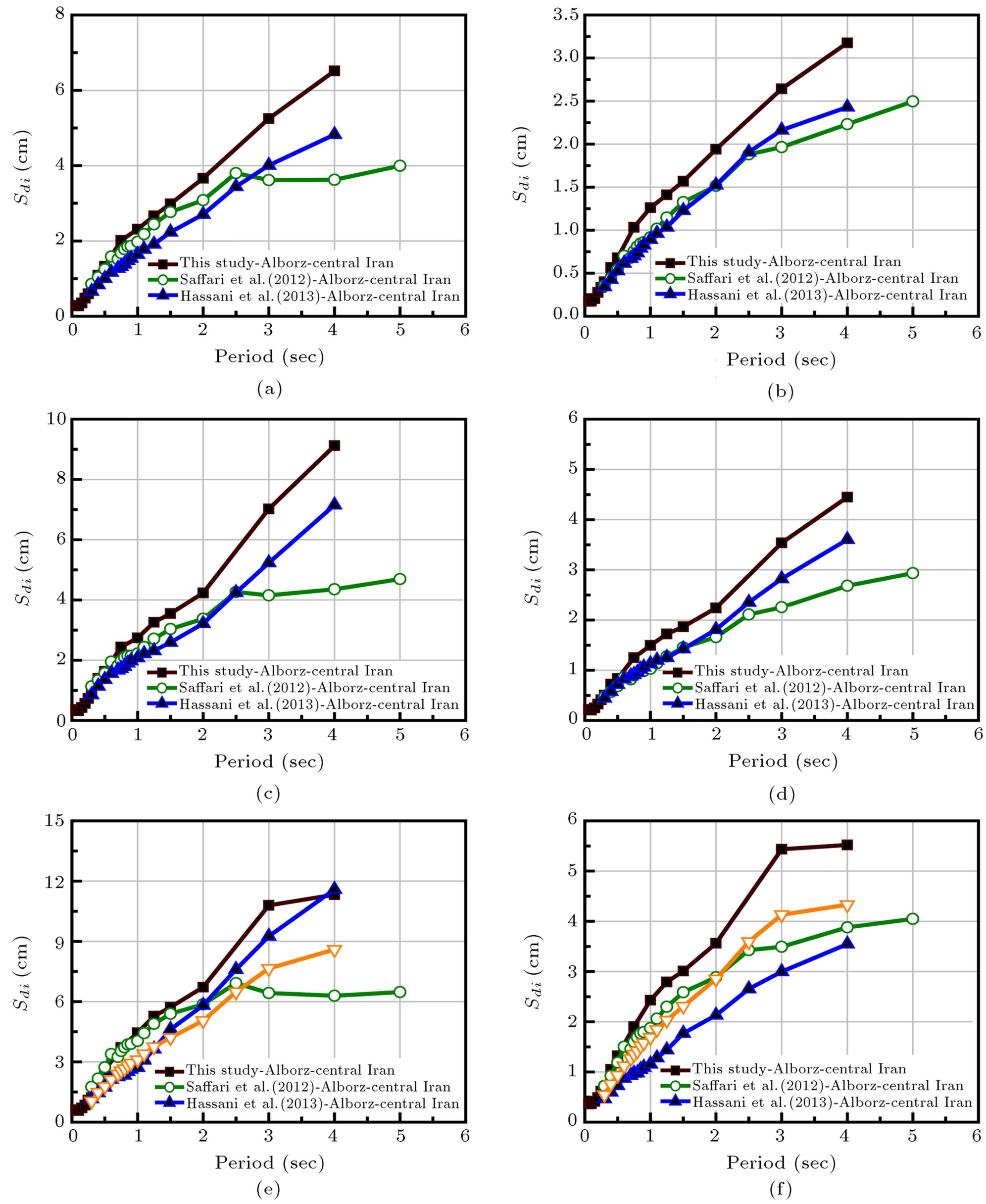

Figure 14. Comparison between equations proposed in this study for Alborz-central Iran and the equation proposed by Tothong and Cornell [2]. The elastic displacement is obtained from various elastic GMPEs (shown in graph). Left-column graphs are for $M_w = 6.5$ and distance of 20 km. Right-column graphs are for $M_w = 6.5$ and distance of 50 Km. In (a) and (b) $V_{30} = 800$ m/sec; in (c) and (d) $V_{30} = 500$ m/sec; and in (e) and (f) $V_{30} = 250$ m/sec. Strength reduction factor is equal to 4. Focal depth is equal to 10 Km.

Zagros zones and Tothong and Cornell model [2] have been presented in Figures 14 and 15. As shown in Figure 14, inelastic displacements, which are estimated by using the Tothong and Cornell [2] model, are lower than the estimated values by the equation proposed in this study for Alborz-central Iran zone.

Based on Figure 15, the model proposed by Saffari et al. [29] is appropriate to estimate inelastic displacement in Zagros region in rock sites.

Hassani et al. [30] used the same dataset to propose a GMPE for elastic spectral acceleration. To find out the reason for the difference between results of the model by Hassani et al. [30] and the equations proposed in this study, we compare the inelastic displacement ratios computed by this study and the model proposed by Tothong and Cornell [2]. Also, the results are compared with the model proposed by Ruiz-García and Miranda [3].

Inelastic displacement ratio, C_R, is defined as the maximum lateral inelastic displacement demand, $\Delta_{\text{inelastic}}$, divided by the maximum lateral elastic displacement demand, Δ_{elastic}, in systems with the same mass and initial stiffness when subjected to the same earthquake ground motion [3]. C_R is defined as:

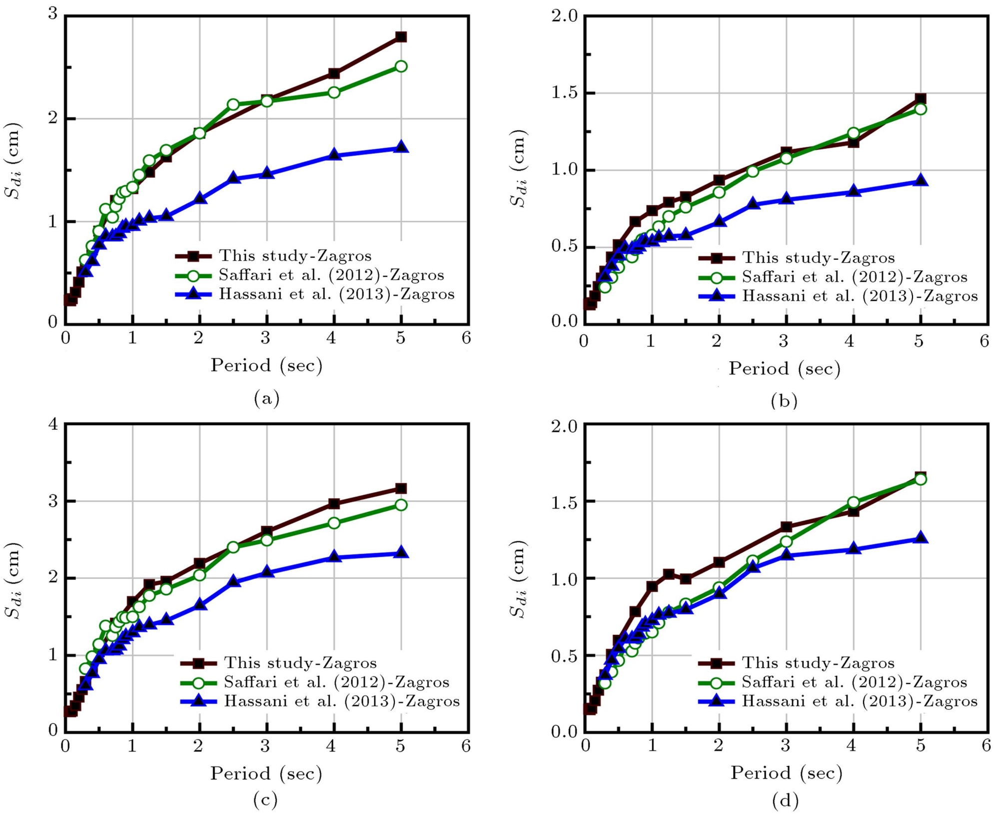

Figure 15. Comparison between equations proposed in this study for Zagros region and the equation proposed by Tothong and Cornell [2]. The elastic displacement is obtained from various elastic GMPEs (shown in graph). Left-column graphs are for $M_w = 6$ and distance of 20 km. Right-column graphs are for $M_w = 6.5$ and distance of 50 km. In (a) and (b) $V_{30} = 800$ m/sec; and in (c) and (d) $V_{30} = 500$ m/sec. Strength reduction factor is equal to 4. Focal depth is equal to 10 km.

$$C_R = \frac{\Delta_{\text{inelastic}}}{\Delta_{\text{elastic}}}. \tag{9}$$

$\Delta_{\text{inelastic}}$ is computed in systems with a constant strength (R).

Inelastic displacement ratio for $M_w = 5.5$, 6.5, and 7 in site conditions 1, 2, and 3 for each model is computed and shown in Figure 16. In Figure 16, strength reduction factors are equal to 4. The results show that inelastic displacement ratios computed by Tothong and Cornell [2] are lower than those by the other models. Thus, this low estimation of inelastic displacement ratio is one of the reasons for the difference between results of this study and Hassani et al. [30] and the other model at high periods. This result is expected because the model of Tothong and Cornell [2] was developed for bilinear oscillators with 5% hardening stiffness ratio.

Also, in this study, curve fitness process is carried out by using the components which have maximum spectral displacement; but, Hassani et al. [30] used geometric mean response spectra of two horizontal components and this is the other reason for the difference between the results of this study and Hassani et al. [30].

7. Conclusion

This paper presents new Ground Motion Prediction Equations (GMPEs) for inelastic spectral displacement in Iran. The proposed relations have been derived based on the records of the earthquakes in Iran and they can be used in both probabilistic and deterministic seismic hazard analyses to create inelastic design spectra, which have several advantages compared to elastic design spectra. The main characteristics of the proposed relations can be listed as follows:

1. The magnitudes of the selected records range from 4 to 7.4 and almost all the earthquakes have epicentral distances less than 200 km;
2. Only a few number of records are for near-fault regions of sever earthquakes. Hence, care should be taken when using them for these regions;
3. Considering seismic tectonic conditions of Iran, three separate GMPEs are presented to compute inelastic spectral displacement for: (a) the whole Iran, (b) Zagros zone, and (c) Alborz-central Iran zone;
4. In Iran's earthquakes catalogues, the specifications

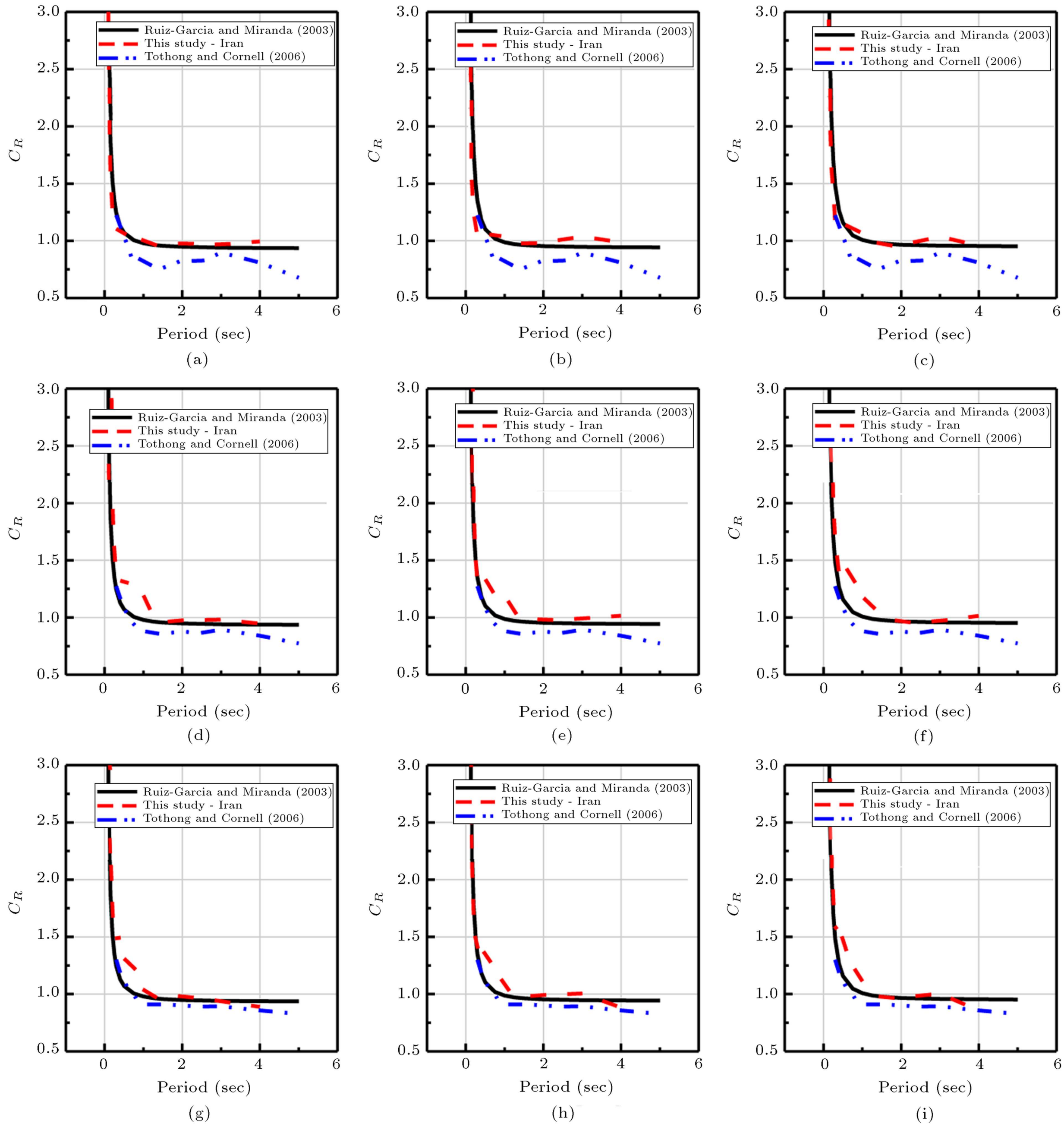

Figure 16. Comparison between inelastic displacement ratios computed by the equation proposed in this study for Iran and the equations proposed by Ruiz-Garcia and Miranda [3] and Tothong and Cornell [2]. In the first row, $M_w = 5.5$, in the second row, $M_w = 6.5$, and in the third row, $M_w = 7$. First-column site: type 1; second-column site: type 2; and third-column site: type 3. Strength reduction factor is equal to 4. Site to source distance is equal to 20 km.

of causative faults have been registered only for a limited number of records. Therefore, fault type and other related parameters have not been considered in the proposed relations.

To evaluate the proposed relations, they have been compared with those proposed by other researchers. There are a few equations for estimation of constant-strength inelastic spectral displacement. The model of Tothong and Cornell [2] is the only one which relates earthquake magnitude to inelastic displacement ratio. In this model, elastic displacement should be estimated by use of elastic GMPE. For comparison, elastic displacement of Tothong and Cornell [2] model is obtained by conducting several elastic GMPEs. The results show the proposed relation for Iran underestimate inelastic spectral displacement in high periods range compared to Campbell and Bozorgnia [26] and Boore and Atkinson [27] in soft soil site condition. Also, it is notable that there is significant difference between the results of this study and Hassani et al. [30]. To explain these differences, inelastic displacement ratio of this study is compared with those of Tothong and Cornell [2] and Ruiz-Garcia and Miranda [3].

However, the compared results for inelastic displacement ratio show a good agreement between the results of this study and the proposed equations by Ruiz-Garcia and Miranda [3]. In addition, it has been found that the values of inelastic displacement ratio computed by Tothong and Cornell [2] are generally lower than the corresponding values obtained by other models. Thus, the underestimation of inelastic displacement ratio could be one of the main reasons for the observed difference between the results of this study and those of Hassani et al. [30]. Also, in this study, curve fitness process has been carried out by using the components with maximum spectral displacement, while Hassani et al. [30] used geometric mean response spectra of two horizontal components.

References

1. Bozorgnia, Y., Hachem, M.M. and Campbell, K.W. "Ground motion prediction equation ("attenuation relationship") for inelastic response spectra", *Earthquake Spectra.*, **26**(1), pp. 1-23 (2010).
2. Tothong, P. and Cornell, C.A. "An empirical ground-motion attenuation relation for inelastic spectral displacement", *Bulletin of the Seismological Society of America.*, **96**(6), pp. 2146-2164 (2006).
3. Ruiz-García, J. and Miranda, E. "Inelastic displacement ratios for evaluation of existing structures", *Earthquake Engineering & Structural Dynamics*, **32**(8), pp. 1237-1258 (2003).
4. Ruiz-García, J. and Miranda, E. "Inelastic displacement ratios for evaluation of structures built on soft soil sites", *Earthquake Engineering & Structural Dynamics*, **35**(6), pp. 679-694 (2006).
5. Miranda, E. "Inelastic displacement ratios for structures on firm sites", *Journal of Structural Engineering*, **126**(10), pp. 1150-1159 (2000).
6. Bozorgnia, Y. Hachem, M.M. and Campbell, K.W. "Deterministic and probabilistic predictions of yield strength and inelastic displacement spectra", *Earthquake Spectra*, **26**(1), pp. 25-40 (2010).
7. Ghodrati Amiri, G., Mahdavian, A. and Dana, F.M. "Attenuation relationships for Iran", *Journal of Earthquake Engineering*, **11**(4), pp. 469-492 (2007).
8. Ghodrati, G., Khorasani, M. and Hessabi, R.M. "Amrei SR ground-motion prediction equations of spectral ordinates and Arias intensity for Iran", *Journal of Earthquake Engineering*, **14**(1), pp. 1-29 (2009).
9. IRCOLD "Relationship between M_s and m_b", Iranian Committee of Large Dams Internal Report (1994) (In Persian).
10. Ambraseys, N.N. and Free, M. "Surface-wave magnitude calibration for European region earthquakes", *Journal of Earthquake Engineering*, **1**(1), pp. 1-22 (1997).
11. Shoja-Taheri, J., Naserieh, S. and Ghofrani, H. "ML and MW scales in the Iranian Plateau based on the strong-motion records", *Bulletin of the Seismological Society of America*, **97**(2), pp. 661-669 (2007).
12. BHRC, *Building and Housing Research Center of Iran Accelerogram Data Bank Web Page*, http://www.bhrc.ac.ir/ (2010).
13. Ambraseys, N., Douglas, J., Sarma, S. and Smit, P. "Equations for the estimation of strong ground motions from shallow crustal earthquakes using data from Europe and the Middle East: horizontal peak ground acceleration and spectral acceleration", *Bulletin of Earthquake Engineering*, **3**(1), pp. 1-53 (2005).
14. BHRC, *Iranian Code of Practice for Seismic Resistant Design of Buildings, Standard No. 2800*, Building & Housing Research Center, 3rd Edn., Tehran, Iran (2005). (In Persian)
15. Zare, M., Bard, P.-Y. and Ghafory-Ashtiany, M. "Site characterizations for the Iranian strong motion network", *Soil Dynamics and Earthquake Engineering*, **18**(2), pp. 101-123 (1999).
16. Sinaeian, F., Zare, M., MirzaiAlavijeh, H. and Farzanegan, E. "Study on site effects and site classification in accelerometric stations", *5th International Conference on Seismology and Earthquake Engineering*, Tehran, Iran (2007) (In Persian).
17. Ghasemi, H., Zare, M., Fukushima, Y. and Sinaeian, F. "Applying empirical methods in site classification, using response spectral ratio (H/V): A case study on Iranian strong motion network (ISMN)", *Soil Dynamics and Earthquake Engineering*, **29**(1), pp. 121-132 (2009).
18. Sinaeian, F., Farzanegan, E. and MirzaeiAlavijeh, H., *Site Geology Investigations in Accelerometric Stations Using Seismic Refraction Method*, Building & Housing Research Center, Tehran, Iran (2010) (In Persian)
19. Zare, M., *Fundamental of Seismic Hazard Analysis*, International Institute of Earthquake Engineering and Seismology, Tehran, Iran (2009) (In Persian).
20. Boore, D.M. and Akkar, S. "Effect of causal and acausal filters on elastic and inelastic response spectra", *Earthquake Engineering & Structural Dynamics*, **32**(11), pp. 1729-1748 (2003).
21. Ghodrati Amiri, G., Zahedi, M., Mahdavian, A. and Gholami, S. "Appropriate frequency band for correcting Iranian accelerograms in different site condition", *Journal of Faculty of Engineering*, University of Tehran, **38**(2), pp. 231-249 (2004) (In Persian).
22. Boore, D.M. and Bommer, J.J. "Processing of strong-motion accelerograms: needs, options and conse-

quences", *Soil Dynamics and Earthquake Engineering*, **25**(2), pp. 93-115 (2005).

23. Akkar, S., Kale, Ö., Boore, D.M., Çektimur, E.V. and Bas, S., *USDP : Utility Software for Data Processing*, METU-Earthquake Engineering Research Center, 1.3.4.21 edn (2011).

24. Abrahamson, N. and Youngs, R. "A stable algorithm for regression analysis using the random effects model", *Bulletin of the Seismological Society of America*, **82**(1), pp. 505-510 (1992).

25. R Development Core Team "R: A language and environment for statistical computing", *R Foundation for Statistical Computing*, Vienna, Austria (2013). url: http://www.R-project.org.

26. Campbell, K.W. and Bozorgnia, Y. "NGA ground motion model for the geometric mean horizontal component of PGA, PGV, PGD and 5% damped linear elastic response spectra for periods ranging from 0.01 to 10 s", *Earthquake Spectra*, **24**(1), pp. 139-171 (2008).

27. Boore, D.M. and Atkinson, G.M. "Ground-motion prediction equations for the average horizontal component of PGA, PGV, and 5%-damped PSA at spectral periods between 0.01 s and 10.0 s", *Earthquake Spectra*, **24**(1), pp. 99-138 (2008).

28. Ghasemi, H., Zare, M., Fukushima, Y. and Koketsu, K. "An empirical spectral ground-motion model for Iran", *Journal of Seismology*, **13**(4), pp. 499-515 (2009).

29. Saffari, H., Kuwata, Y., Takada, S. and Mahdavian, A. "Updated PGA, PGV, and spectral acceleration attenuation relations for Iran", *Earthquake Spectra*, **28**(1), pp. 257-276 (2012).

30. Hassani, N., Ghodrati Amiri, G., Bararnia, M. and Sinaeian, F. "Ground motion prediction equation (attenuation relationship) for spectral acceleration in Iran", *Sharif Journal of Science & Technology*, **31**(2), pp. 11-21 (2015) (In Persian).

31. Shoja-Taheri, J., Naserieh, S. and Hadi, G. "A test of the applicability of NGA models to the strong ground-motion data in the Iranian plateau", *Journal of Earthquake Engineering*, **14**(2), pp. 278-292 (2010).

Biographies

Nemat Hassani graduated from Amirkabir University with both BS and MS degrees in Civil and Structural Engineering. He received his PhD degree from Kobe University (Japan) doing on Lifelines Earthquake Engineering, experiencing 1995 Kobe Earthquake.

Dr. Hassani was an Assistant Professor at Kobe University and now is an Assistant Professor and Dean of Civil, Water & Environmental Engineering Department at Shahid Beheshti University (SBU) in Tehran, Iran. His main fields of research are earthquake engineering and disaster management.

Gholamreza Ghodrati Amiri is a faculty Professor at the School of Civil Engineering, Iran University of Science and Technology, Tehran, Iran. His current research interests include seismic hazard analysis and random vibrations, damage detection and health monitoring, and probabilistic seismic assessments of structures and bridges.

Majid Bararnia is PhD candidate in the Department of Civil, Water & Environmental Engineering at Shahid Beheshti University, Tehran, Iran. His research activities have included studies of dynamic soil-structure interaction, seismic hazard analysis, seismic design, and assessments of bridges.

Fereydoon Sinaeian graduated from IIEES in Seismology and continued his research works at BHRC as the director of Iran Strong Motion Network. His main field of research is seismic attenuation. He is now doing consultancy in some companies in Canada.